Nonlinear magnetoacoustics of orthoferrite near spin flip

A. Yu. Lebedev, V. I. Ozhogin, V. L. Safonov, and A. Yu. Yakubovskiĭ

I. V. Kurchatov Institute of Atomic Energy
(Submitted 11 March 1983)

Second harmonic generation by a transverse ultrasonic wave of frequency 38 MHz is investigated both experimentally and theoretically for the case of an antiferromagnet with spin flip (TmFeO$_3$). The efficiency $u_{2\omega}/u_\omega$ for transformation of the fundamental into the second harmonic increases strongly upon approach to the spin-flip region from the symmetric phase side, and reaches $\sim 20\%$ for a strain $u_\omega \sim 10^{-5}$. At higher strain $(u_\omega > 3 \times 10^{-5})$, an anomalous behavior of the second-harmonic signal is observed. This can apparently be ascribed to its reaction on the initial sound wave. By precise orientation of the magnetic field (accurate to $\pm 5'$), it was possible to discern and investigate two mechanisms of effective acoustic nonlinearity. One is related to the "purely magnetic" anharmonicity of the spin system, and the other to the nonlinearity of the magnetoelastic coupling.

PACS numbers: 43.35.Rw, 75.80. + q, 75.50.Ee

1. INTRODUCTION

Intensive experimental investigation of the nonlinear acoustic phenomena at ultrasonic frequencies in magnetic crystals has been stimulated by Refs. 1 and 3, in which a large value of the elastic anharmonism was predicted in antiferromagnets (AF) with magnetic anisotropies of the easy plane type. The magnetoelastic dynamical nonlinearity can be large even in the hypersonic range of frequencies[3] if the point of intersection of the spectra of magnons and phonons falls in this region—the so-called magnetoacoustic resonance. The nature of the anharmonism in both cases is due to a significant nonlinearity introduced into the elasticity by the magnetic subsystem via the magnetostrictive interaction. It turns out here that the effective third-order elastic moduli C_3^{eff} can be 10^3 times (or more) greater than the ordinary values of the purely elastic nonlinearity for solids, and depend strongly on the external magnetic field (and also on the external mechanical stresses). It follows from theory[1,2] that the nonlinearity of the ultrasonic magnetoelastic waves should be especially large in an AF with a large exchange field H_E and with low ("soft") frequency of antiferromagnetic resonance (AFMR). The best known example of such AF is hematite (α-Fe$_2$O$_3$) in its easy-plane phase $(T_M < T < T_N)$, for which different nonlinear acoustic effects are observed: doubling of the frequency and acoustic sound detection,[4] self-action[5] and nonresonant interaction[6] of sound waves, stimulated Raman scattering of sound.[7]

The presence of a soft mode of AFMR is characteristic not only for easy-plane AF, but also for crystals experiencing a second order spin-flip phase transition. In these materials, for example, in rare-earth (R) orthoferrites RFeO$_3$, there are additional possibilities of the action on the nonlinearity by such parameters as the direction of the magnetic field and the temperature. For the study of these possibilities, we have investigated the simplest of nonlinear effects—the doubling of the sound frequency—in a single crystal of thulium orthoferrite (TmFeO$_3$). This system has a spin-flip temperature range 82–94 K that is convenient for experimentation, and

the sound velocity changes in it significantly in this range.[8] The latter suggests the possibility a large values of the nonlinear acoustic effects.

The spin flip in orthorhombic TmFeO$_3$ takes place in the absence of a magnetic field **H** in the following way. The antiferromagnetism vector **l** is directed at temperatures $T < T_1 = 82$ K along the c axis of the crystal (the c phase) and at $T > T_2 = 94$ along the a axis (a phase). In the intermediate temperature range $T_1 < T < T_2$, the vector **l** rotates smoothly from one of these axes to the other (ac phase). At $H = 0$, the temperatures T_1 and T_2 are points of second-order phase transitions.

The tensor of linear elastic moduli $\hat{C}_2$ and the spectrum of the AFMR thulium orthoferrite have been investigated in detail in Refs. 8–12; in this case, a significant change in $\hat{C}_2$ was observed near the phase transitions. This change is connected with the appearance of magnetoelastic interaction under conditions of softening of one of the magnetic modes.[8] In TmFeO$_3$, as also in other rare-earth orthoferrites with a high Néel temperature T_N, the magnetic subsystem is "more stiffly" elastic, i.e., the maximum velocity of the magnons is larger than the sound velocity. Therefore, near the phase-transition points, the condition of magneto-acoustic resonance is satisfied for sufficiently low sound frequencies. Preliminary experimental results, indicating a large acoustical nonlinearity in TmFeO$_3$ near the spin reorientation, were published by us previously.[13]

2. EXPERIMENTAL METHOD

The sample of TmFeO$_3$ was cut from a single crystal grown in the Moscow Power Institute by the method of crucible-free zone melting with radiation heating, and had the shape of a prism of cross section 6×6 and length 12 mm along the a axis of the crystal. To decrease the inhomogeneity of the magnetic field inside the sample ($\mathbf{H} \perp a$), its edges were rounded off along the entire length at a radius of 4 mm.

The excitation and detection of transverse sound with a wave vector $\mathbf{k} \| a$ were accomplished by attaching identical

piezotransducers at the opposite ends of the sample. Each transducer consisted of a plate of X-cut $LiNbO_3$, thickness $50\,\mu$, glued by means of a thin layer of low-temperature epoxy resin DFM-135 to a molybdenum-glass substrate into which was soldered a molybdenum electrode of 2 mm diameter which determined the cross section of the sound beam. A niobium film of thickness $0.5\,\mu$ served as the second electrode. It was deposited by cathode sputtering on the surface of the holder with the plate. Niobium was chosen because of its high adhesiveness and mechanical strength. Thanks to the large electromechanical coupling constant that is characteristic of lithium niobate, the described converter has an appreciable bandwidth.[14] In our case the double-conversion losses amounted to 22 dB at a frequency of 33 MHz for the primary wave and 70 dB for the frequency of the second harmonic. The acoustical contact between the transducer and the sample was achieved by means of a thin layer of Apiezon-N vacuum grease. The error in the setting of the polarization of the transducers relative to the axes of the sample did not exceed 5°.

The echo-pulse method of measurement ("in transmission") was employed with a pulse duration $\tau \sim 1\,\mu$s and repetition rate ~ 100 Hz. The signal of the supply HF generator was amplified to a level of ~ 100 W and fed to the input transformer through a second-harmonic filter and a loop matching transformer. The second harmonic appearing in the sample was recorded by the output transducer and by a receiver with a bandwidth of 4 MHz, while the detected signal was observed on the screen of an oscilloscope. The magnetic field was produced by an electromagnet placed on a rotatable platform, the axis of rotation of which could be inclined by several degrees from the vertical in two mutually perpendicular planes. The field was set with an error not exceeding 5′ with respect to the crystallographic axes. The supply system of the magnet assured a field stability $\sim 2 \times 10^{-4}$. The temperature of the sample was kept constant in the range 65–130 K by a precision thermoregulator with a relative error of less than 1 mK. The absolute error of measurement of the temperature did not exceed 1 K. Local overheating of the sample by the sound pulses did not exceed 2 mK.

3. EXPERIMENTAL RESULTS

Doubling of the ultrasonic frequency at $H = 0$

Before investigating the behavior of the second harmonic of the sound in the spin-flip region it was necessary to determine very accurately the temperatures T_1 and T_2 of the transitions in the absence of the field. For this purpose, we used the well-known increase of the sound attenuation at the point of the spin-flip phase transition.[15] Far from the region of spin flip, the observed series of the fundamental-frequency echo signal was ideal and up to 100 pulses could be recorded (quality factor of the wave was $\gtrsim 10^4$). When the temperatures T_1 or T_2 were approached (from below and above respectively) the sound absorption increased abruptly (Fig. 1a), so that the temperatures of the transitions could be recorded with an error of not greater than 10 mK. Near the transitions, the envelope of the echo series differed signifi-
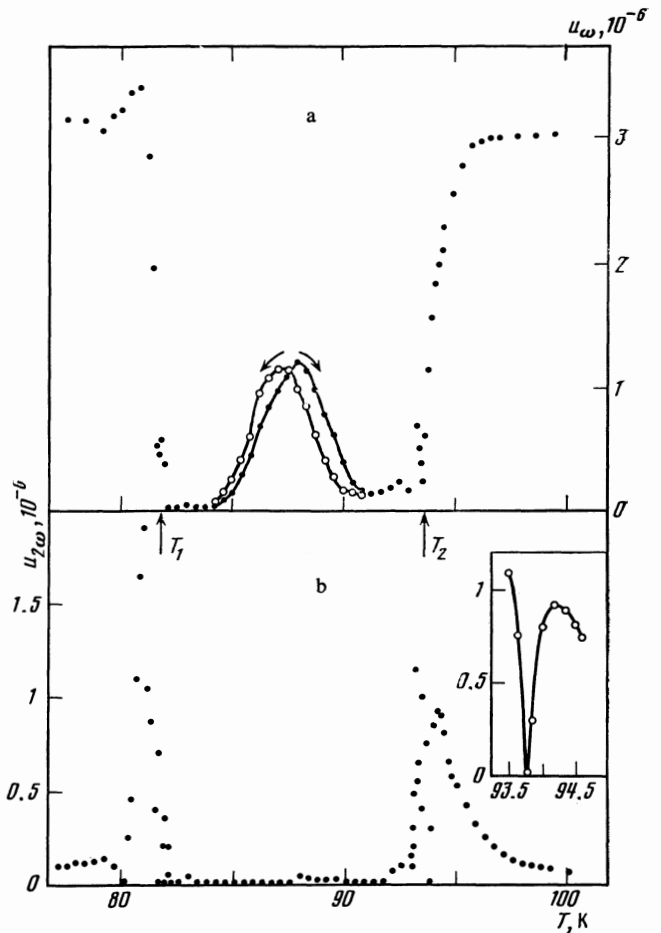

FIG. 1. Temperature dependences of the fundamental-frequency signal u_ω passing through the sample (a) and the amplitude of the second-harmonic signal $u_{2\omega}$ (b) at $\mathbf{H} = 0$. The inset shows the region of transition T_2 with tripled temperature scale.

cantly from exponential; in fact, just as in Ref. 8, a modulated series was observed with a temperature-dependent shape of the envelope. Therefore, for measurement of the sound attenuation, we used the amplitude of only the first sound transmitted pulse.

In temperature intervals of width ~ 3 K adjoining T_1 or T_2 from the side of the ac-phase, irregular jumps in the signal were observed, evidently due to the presence of a domain structure. The temperature hysteresis of the observed sound absorption in the ac-phase (see Fig. 1a) is probably also due to the domain structure, while the smoothness of the plot of the signal of fundamental frequency $u_\omega(T)$ that passed through the sample, in the center of the ac-phase, can be due to coupling of the magnetic and elastic subsystems, which in the given method obviously masks the jumps of the domain boundaries, and which is weak for the given region. A detailed study of these questions was not our intention. All the subsequent study of the acoustic nonlinearity was carried out only for the a- and c-phases.

A second-harmonic signal is practically absent from the spin-flip region. This indicates both a weak coupling of the magnetic and elastic waves at these temperatures, and a
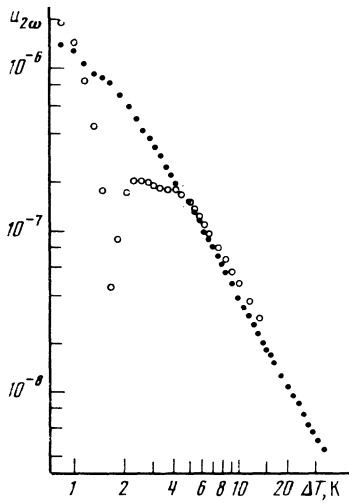
FIG. 2. Temperature dependences of the amplitude of the second harmonic near the spin-flip region at $H = 0$; O—low-temperature phase, $1 \parallel c$, ●—high-temperature phase, $1 \parallel a$; $u_\omega \approx 3 \times 10^{-6}$.

small natural anharmonism of the elastic subsystem. As the temperature of reorientation is approached, the signal increases approximately in proportion to ΔT^{-2}, where $\Delta T = T - T_2$ in the a-phase and $\Delta T = T_1 - T$ in the c-phase (Fig. 2). At the point of the deep minimum of the $u_{2\omega}$ (T) curve (see Fig. 2, $\Delta T \approx 2$ K, and also Fig. 1, $T \approx 80$ K) the temporal phase of the second harmonic presumably changes by π judging from the behavior of the envelope of the signal on the screen of the oscilloscope.

Doubling of the ultrasonic frequency at $H \neq 0$.

Upon superposition of an external magnetic field of arbitrary direction, the a- and c-phases are mixed, none of the phase transition is realized in pure form, and a soft mode does not develop in the system. The nonlinear acoustic effects are small here. But if the field $\mathbf{H}$ is directed strictly along the c axis, only the c-phase vanishes,[11] but the $a–ac$ phase transition remains. The temperature T_2^* at which the transition occurs depends on the value of $\mathbf{H}$ in the following way:$T_2^* = T_2 + \beta_2 H_c$.[11] A similar situation occurs in the case $\mathbf{H} \parallel a$ for the $c–ac$ transition; here $T_1^* = T_1 + \beta_1 H_a$. The coefficients β_1 and β_2, which we determined from the data of the temperature measurements of the sound attenuation in the region of phase transitions (see the previous section) at different external fields, amounted to 0.56 deg/kOe and $- 0.68$ deg/kOe, respectively. The temperatures T_1^* and T_2^* of the phase transitions do not depend on the projection H_b of the external field on the b axis of the crystal, within the limits of accuracy of our experiment.

The most characteristic feature of the acoustic nonlinearity that arises upon the application of the external field is that the amplitude $u_{2\omega}$ of the second-harmonic signal experiences the increment $\tilde{u}_{2\omega}$, which is an odd function of H_b. In the study of this incremental signal, we must distinguish it against the background of the initial signal that exists without the field. The measurement procedure in the a-phase reduces to the following: the value of the signal $u_{2\omega}$ is deter-
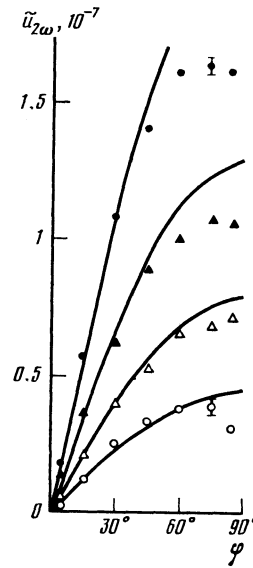

FIG. 3. Angular dependences of the second harmonic signal $\tilde{u}_{2\omega}$ in the high-temperature phase $(\Delta T = 4$ K) at $u_\omega = 6 \times 10^{-7}$ for several values of the field: ●—$H = 4.5$ kOe; ▲—$H = 3$ kOe; △—$H = 2$ kOe; O—$H = 1.4$ kOe.

mined in the field $(0, H_b, H_c)$; then the field is rotated in the (bc) plane and the signal is measured in the field $(0, - H_b, H_c)$. The half-difference $\tilde{u}_{2\omega}$ of these signals represents in pure form the manifestation of a second-harmonic generation mechanism that depends on the external field. In the c-phase, the measurements were carried out in similar fashion; however, the field was rotated in the (ab) plane from a value $(H_a, H_b, 0)$ to $(H_a, - H_b, 0)$.

We have studied the dependence of the signal $\tilde{u}_{2\omega}$ of the second harmonic on the value of the magnetic field and its direction in the (bc) plane, which is set by the angle φ measured from the c axis, with the amplitude of the strain in the primary wave kept constant. The angular dependences shown in Fig. 3 are well approximated by the curve $\tilde{u}_{2\omega} \propto H_b = H \sin \varphi$ in the range of fields $H < 2$ kOe. In a narrow range of angles ($\pm 5°$) near $\varphi = 90°$, a sharp decrease in signal was observed, which can be attributed to the onset of weakly ferromagnetic domains at $H_c = 4\pi M_0 \, m_z^{(0)} \approx 70$ Oe. The walls of these domains absorb and scatter the sound strongly. The experimental dependences of the signal $\tilde{u}_{2\omega}$ on magnetic field at fixed values of the angle φ (Fig. 4) are described by an expression of the form $\tilde{u}_{2\omega} \propto H^{1.2}$ in the range of fields 0.7–4.5 kOe. It was also possible for us to investigate the dependence of $\tilde{u}_{2\omega}$ on the temperature of the sample. As follows from Fig. 5, the growth of the signal $\tilde{u}_{2\omega}$ as one approaches the temperature T_2 follows a $(T - T_2)^{-3}$ law. Departure from the $(T - T_2)^{-3}$ law begins at $T - T_2 \lesssim 4$ K and is probably due to the gradual inclusion of magnetoelastic damping.[13,14]

Measurements in the c-phase show that the dependences of $\tilde{u}_{2\omega}$ on H and T are similar to those obtained for the a-phase. However, the effectiveness of conversion into the second harmonic is approximately half as great.
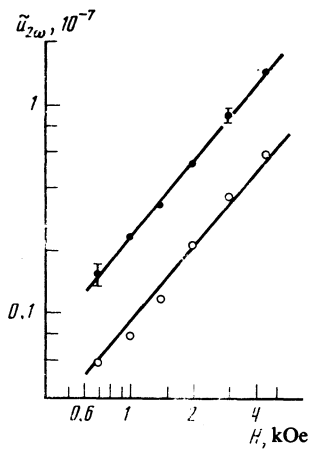
FIG. 4. Dependences of the second-harmonic signal $\tilde{u}_{2\omega}$ in the high-temperature phase ($\Delta T = 4$ K) on the value of the field at $u_\omega = 6 \times 10^{-6}$ for two values of the angle φ: ●—45°, ○—15°.

FIG. 6. Amplitude dependences of the strain $\tilde{u}_{2\omega}$ in the high-temperature phase: $H = 4.5$ kOe, $\varphi = 45°$, △—$\Delta T = 5$ K, ○—$T = 1.7$ K; ●—$T = 0.2$ K.

In the measurement of the efficiency of conversion of the primary wave into its second harmonic, the absolute value of the strain u_ω in the primary wave is determined by the relation

$$u_\omega = (Q/2\rho v_s^3)^{1/2}, \tag{1}$$

where $Q = (P_{inc} - P_{refl})\beta S$; P_{inc} and P_{refl} are the HF powers incident on and reflected from the transducer; β is the coefficient of electromechanical conversion; S is the cross section of the sound beam; ρ is the density of the crystal, and v_s is the speed of sound. To find the strain $u_{2\omega}$ in the wave of the second harmonic, a calibration of the detecting transducer was carried out. In this case, this transducer operated in the "reflection" mode. Measurement of the electric parameters contained in (1), and also of the output signal of the detector, enabled us to determine the sensitivity of the receiving channel of the apparatus to the strain $u_{2\omega}$. The conversion efficiency $u_{2\omega}/u_\omega$ measured in this way at $u_\omega \equiv u \approx 6.10^{-6}$, $\Delta T = 4K$ and $H_b = 3$ kOe amounted to $\sim 3\%$.

4. STRONG NONLINEARITY

All the results given above were obtained in the region of weak nonlinearity, i.e., at $u_{2\omega} \ll u_\omega$. The reserve power at our disposal enabled us to proceed to the region of strong nonlinearity, where $u_{2\omega} \sim u_\omega$. Figure 6 shows the amplitude dependence of the second harmonic signal for several temperatures; here the level of input HF power was set by a calibrated attenuator, and a similar attenuator maintained the signal at the input of the detector at a constant value, thus eliminating a possible nonlinearity of the receiving channel of the apparatus. Far from the a–ac transition (curve 1), the quadratic dependence $u_{2\omega} \propto u_\omega^2$, which is typical of the regime of weak nonlinearity, was satisfied up to the maximum strains achieved. As the transition point was approached, departure from this law was observed initially (curve 2), and then an anomalous behavior of the second-harmonic signal (curve 3). The anomaly consisted of an initial deep minimum in the signal at large strains u_ω, and the echo pulses observed here had a strongly distorted shape (see Fig. 7).

5. THEORY

Rare-earth orthoferrites constitute AF with four sublattices formed by the ions Fe^{3+}; however, the basic properties of these AF are frequently described within the framework of a model with two sublattices M_1 and M_2. The energy density W is written down in the form of a sum of the densities of the kinetic energy due to the variable part of the elastic displacement U, the potential energy density F, and the Zeeman energy density:

$$W = {}^1\!/_2\rho\dot{U}^2 + F - 2M_0(mH).$$

The potential energy density includes the magnetic F_m, the elastic F_e and the magnetoelastic F_{me} components: $F = F_m + F_e + F_{me}$. For orthoferrite crystals (space group D_{2h}^{16}) each component can be represented in the form
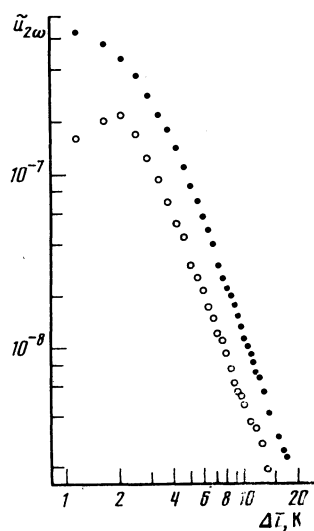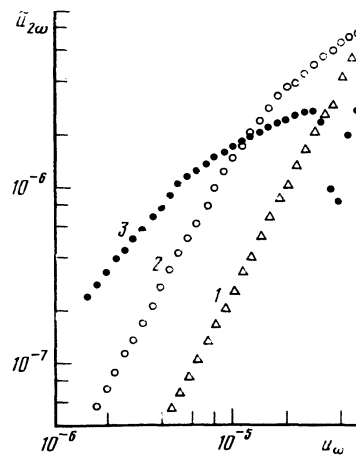

FIG. 5. Temperature dependences of the second harmonic signal $\tilde{u}_{2\omega}$ in the high-temperature phase: $u_\omega \approx 6 \times 10^{-6}$, $\varphi = 45°$; $1 \parallel a$: ○—$H = 2$ kOe, ●—$H = 4.5$ kOe.
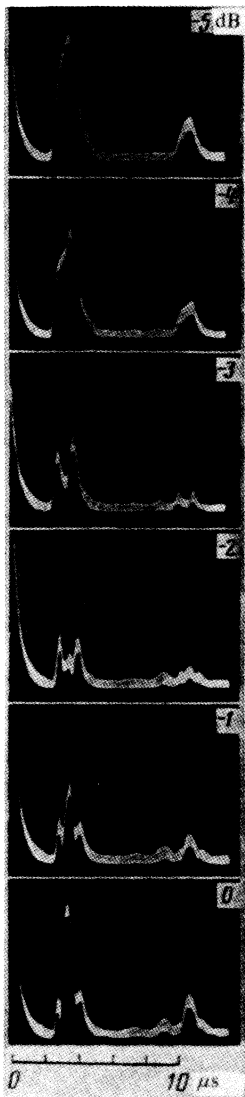
FIG. 7. Oscillograms of the second-harmonic signal (the first two pulses of the echo series), obtained under various conditions of input HF power and corresponding to the anomalous segment of curve 3 on Fig. 6 at the power level 0 dB, the strain is $\sim u_\omega \approx 5 \times 10^{-5}$.

$$F_m = 2M_0(H_E m^2 + D_1 m_x l_z - D_3 m_z l_x + \tfrac{1}{2} A_1 l_x^2$$
$$+ \tfrac{1}{2} C_1 l_z^2 + \tfrac{1}{4} A_2 l_x^4 + \tfrac{1}{4} C_2 l_z^4 + \tfrac{1}{2} G l_x^2 l_z^2), \qquad (2a)$$

$$F_e = \tfrac{1}{2}(C_{11} u_{xx}^2 + C_{22} u_{yy}^2 + C_{33} u_{zz}^2) + C_{12} u_{xx} u_{yy} + C_{13} u_{xx} u_{zz}$$
$$+ C_{23} u_{yy} u_{zz} + 2C_{44} u_{yz}^2 + 2C_{55} u_{xz}^2 + 2C_{66} u_{xy}^2, \qquad (2b)$$

$$F_{me} = 2[(B_{11} u_{xx} + B_{12} u_{yy} + B_{13} u_{zz})l_x^2 + B_{55} u_{xz} l_x l_z$$
$$+ (B_{21} u_{xx} + B_{22} u_{yy} + B_{23} u_{zz})l_y^2 + B_{66} u_{xy} l_x l_y$$
$$+ (B_{31} u_{xx} + B_{32} u_{yy} + B_{33} u_{zz})l_z^2 + B_{44} u_{yz} l_y l_z]. \qquad (2c)$$

Here ρ is the density of the crystal; $\mathbf{m} = \mathbf{m}_1 + \mathbf{m}_2$; $\mathbf{l} = \mathbf{m}_1 - \mathbf{m}_2$; $\mathbf{m}_j = \mathbf{M}_j/2|\mathbf{M}_j|$, $|\mathbf{M}_j| = M_{j0}$ are the values of the magnetization of the sublattices ($j = 1,2$); H_E is the exchange field; D_1 and D_2 are the Dzyaloshinskiĭ fields; A_1, C_1 and A_2, C_2, G the fields of the bilinear and biquadratic anisotropies; C_{ij} and B_{ij} are the elastic and magnetoelastic moduli. The coordinate axes x, y, z are directed along the axes a,b,c,

respectively, of the crystal. The elastic anharmonism proper is not taken into account in Eqs. (2b), since, under the conditions of our experiment, it turns out to be small in comparison with the anharmonism introduced into the elastic system by the magnetic system. For this same reason, we can neglect the geometric nonlinearity in the strain tensor u_{ik} and take

$$u_{ik} = \tfrac{1}{2}(\partial U_i/\partial x_k + \partial U_k/\partial x_i).$$

We shall carry out calculations as applied the experiment described above for the case of the $a(\Gamma_4)$-phase in the field $\mathbf{H} = (0, H_y, H_z)$. The calculation for the $c(\Gamma_2)$-phase is analogous and differs from the a-phase only in the notation (Γ_2 and Γ_4 are defined, for example, in Ref. 9).

It is convenient to go from the variables $\mathbf{m}$ and $\mathbf{l}$ in Eqs. (2) to the new variables

$$\mathcal{M}^\alpha = m_1^{\alpha_1} + m_2^{\alpha_2}, \quad \alpha = \xi, \eta, \zeta,$$
$$\mathcal{L}^\alpha = m_1^{\alpha_1} - m_2^{\alpha_2}, \quad \alpha_\nu = \xi_\nu, \eta_\nu, \zeta_\nu, \quad \nu = 1, 2. \qquad (3)$$

The quantities $m_1^{\alpha_1}$ and $m_2^{\alpha_2}$ are the components of the vectors $\mathbf{m}_1$ and $\mathbf{m}_2$ in the "intrinsic" set of coordinates bound to the equilibrium directions of the magnetizations $\mathbf{M}_{10}$ and $\mathbf{M}_{20}$, while the axes ζ_1 and ζ_2 are directed along $\mathbf{M}_{10}$ and $\mathbf{M}_{20}$, respectively.

The transition from the x, y, z representation to the ξ, η, ζ representation is realized by a transformation consisting of two rotations:

$$m_\nu^x = \pm m_\nu^{\xi_\nu} \cos\theta - m_\nu^{\eta_\nu} \sin\theta,$$
$$m_\nu^y = m_\nu^{\xi_\nu} \cos\psi - (m_\nu^{\xi_\nu} \sin\theta \pm m_\nu^{\eta_\nu} \cos\theta)\sin\psi, \qquad (4)$$
$$m_\nu^z = m_\nu^{\xi_\nu} \sin\psi + (m_\nu^{\xi_\nu} \sin\theta \pm m_\nu^{\eta_\nu} \cos\theta)\cos\psi.$$

The upper sign in (4) corresponds to the transformation $x, y, z \to \xi_1, \eta_1, \zeta_1$; the lower corresponds to $x, y, z \to \xi_2, \eta_2, \zeta_2$. The usual normalization conditions

$$(\mathbf{m}, \mathbf{l}) = 0, \quad \mathbf{m}^2 + \mathbf{l}^2 = 1 \qquad (5)$$

for the variables $m_\nu^{\alpha_\nu}$ take on the form

$$(m_\nu^{\xi_\nu})^2 + (m_\nu^{\eta_\nu})^2 + (m_\nu^{\zeta_\nu})^2 = \tfrac{1}{4}, \quad \nu = 1, 2. \qquad (6)$$

It is evident that the small oscillations of the components $m_\nu^{\zeta_\nu}$ are quadratic in $m_\nu^{\xi_\nu}$; and $m_\nu^{\eta_\nu}$; therefore, the condition (6) is conveniently rewritten in the form

$$m_\nu^{\zeta_\nu} = [\tfrac{1}{4} - (m_\nu^{\xi_\nu})^2 - (m_\nu^{\eta_\nu})^2]^{1/2} \approx \tfrac{1}{2} - (m_\nu^{\xi_\nu})^2 - (m_\nu^{\eta_\nu})^2. \qquad (7)$$

Thus, the expression for the energy density can be written with the help of (7) in the form of a function $W(\mathcal{M}^\xi, \mathcal{M}^\eta, \mathcal{L}^\xi, \mathcal{L}^\eta)$ of four (instead of the initial six) "magnetic" variables. From the equilibrium conditions

$$\frac{\partial W}{\partial \mathcal{M}^\xi} = \frac{\partial W}{\partial \mathcal{M}^\eta} = \frac{\partial W}{\partial \mathcal{L}^\xi} = \frac{\partial W}{\partial \mathcal{L}^\eta} = 0 \qquad (8)$$

it is not difficult to obtain the equilibrium values of the cant angles, which in the case of a weak magnetic field ($H \ll 2H_E$) are

$$\theta \approx (H_z + D_3)/2H_E, \quad \psi \approx -H_y/(D_3 + H_z). \qquad (9)$$

The quadratic part $F_m^{(2)}$ of the magnetic energy density has in the notation of (3) the form

$$F_m^{(2)}$$

$$=2M_0\{[H_E(1-\theta)^2+D](\mathcal{M}^\xi)^2+(\tfrac{1}{2}C_1+\tfrac{1}{2}G+D-D_1\theta)(\mathcal{M}^\eta)^2$$

$$-(H_E\theta^2-D)(\mathcal{L}^\xi)^2$$

$$+[H_E(1-2\theta^2)+D_3\theta+D](\mathcal{L}^\eta)^2+\psi(C_1+2G)\mathcal{M}^\eta\mathcal{L}^\xi\}, \quad (10)$$

where

$$D\equiv(D_3+\tfrac{1}{2}H_z)\theta-\tfrac{1}{2}(A_1+A_2).$$

It is seen that in the case $H_y=0$ ($\psi=0$) the variables separate. Equation (10) can be further simplified by transition to the Hamiltonian variables (such an approach is completely analogous to second quantization):

$$a=\mathcal{M}^\xi+i\mathcal{M}^\eta, \quad a^*=\mathcal{M}^\xi-i\mathcal{M}^\eta,$$

$$b=\mathcal{L}^\xi+i\mathcal{L}^\eta, \quad b^*=\mathcal{L}^\xi-i\mathcal{L}^\eta \quad (11)$$

followed by diagonalizations with the help of the u,v transformation

$$a=u_1c+v_1c^*, \quad b=u_2d+v_2d^*.$$

The quadratic form (10) becomes

$$F_m^{(2)}=2M_0(\Omega_1c^*c/\gamma+\Omega_2d^*d/\gamma), \quad (12)$$

where

$$\Omega_1=\gamma[H_z(H_z+D_3)+2(D_3-D_1)(H_z+D_3)$$

$$+2H_E(C_1+G-A_1-A_2)+\Omega_{1mes}^2]^{1/2},$$

$$\Omega_2=\gamma[(2D_3+H_z)(D_3+H_z)-2H_EA_2+\Omega_{2mes}^2]^{1/2} \quad (13)$$

are the frequencies of the quasiferro- and quasiantiferromagnetic branches, respectively, of the spin-wave spectrum; γ is the magnetomechanical ratio; $\Omega_{1\,mes}$ and $\Omega_{2\,mes}$ are the magnetoelastic gaps in the spectrum of the spin waves for which expressions are given in Ref. 16.

The variables $\mathcal{M}^\alpha$, $\mathcal{L}^\alpha$ are expressed in terms of c,c^* and d,d^* in the following fashion:

$$\mathcal{M}^\xi\approx(\Omega_1/8\gamma H_E)^{1/2}(c+c^*), \quad \mathcal{M}^\eta\approx-i(\gamma H_E/2\Omega_1)^{1/2}(c-c^*),$$

$$\mathcal{L}^\xi\approx(\gamma H_E/2\Omega_2)^{1/2}(d+d^*), \quad \mathcal{L}^\eta\approx-i(\Omega_2/8\gamma H_E)^{1/2}(d-d^*). \quad (14)$$

The quasiferromode of the spin waves is strongly connected with the sound, since this mode softens at the point of the a-c phase transition. The upper branch of the spin waves, remaining of high frequency, is weakly coupled with the sound; however, in the presence of the component H_y of the external field, the modes become mixed, and this can be reflected in the character of the dynamical magnetoelastic coupling.

The inequality $\Omega_1^2>\Omega_{1\,mes}^2$ is the stability condition for the considered magnetic field (1 $\|a$), while the point $\Omega_1=\Omega_{1mes}$ corresponds to the a-ac phase transition, since this is a second-order transition. The linear magnetoelastic dynamics of the orthoferrite at $\mathbf{H}=0$ was investigated theoretically in detail in Ref. 16. In the presence of the field $\mathbf{H}=(0,H_y,H_z)$, the temperature T_2 of the a-ac transition is shifted:

$$T_2(H)=T_2(0)-(3D_3-2D_1)/2H_E\frac{\partial}{\partial T}(C_1-A_1), \quad (15)$$

while the c-ac phase transition vanishes as such, since the symmetry of the system is the same on both sides of $T_1(0)$ at $H_z\neq0$. The equation for the speed of the sound-like wave (with polarization u_{xz}) in the a-phase, obtained in Ref. 16 and given by

$$v_s=\left[\frac{C_{55}}{\rho}\left(1-\frac{H_EB_{55}^2}{M_0C_{55}(\Omega_1/\gamma)^2}\right)\right]^{1/2}\equiv\left(\frac{\bar{C}_{55}}{\rho}\right)^{1/2}, \quad (16)$$

remains valid also at $H=(0,H_y,H_z)$ if we can write the AFMR frequency entering into it in accord with (13).

The nonlinear phenomena of the considered system at low (ultrasonic) frequencies are due to the anharmonism of the magnetoelastic coupling of the form

$$F_{me}^{(2)}=2[(B_{31}-B_{11})u_{xx}+(B_{32}-B_{12})u_{yy}+(B_{33}-B_{13})u_{zz}](\mathcal{M}^\eta)^2. \quad (17)$$

Because of the linear magnetoelastic coupling, which has the energy

$$F_{me}^{(1)}=2B_{55}u_{xz}\mathcal{M}^\eta, \quad (18)$$

the variable strain u_{xz} excites nonresonantly oscillations of the variable quasiferromode (since the ultrasonic frequencies are much smaller than those of the spin waves). From the condition $\partial F/\partial\mathcal{M}^\eta=0$ it is not difficult to obtain

$$\mathcal{M}^\eta=-B_{55}(\gamma/\Omega_1)^2(H_E/M_0)u_{xz}. \quad (19)$$

Substituting (19) in (17), we find that the magnetoelastic coupling leads to the effective nonlinearity in the elastic subsystem

$$F_{eff}=2B_{55}^2(\gamma/\Omega_1)^4(H_E/M_0)^2[(B_{31}-B_{11})u_{xx}$$

$$+(B_{32}-B_{12})u_{yy}+(B_{33}-B_{13})u_{zz}]u_{xz}^2. \quad (20)$$

As applied to the experiment described above, let us consider an initial sound wave polarized along the z axis, with frequency $\omega\ll\Omega$ and wave vector $\mathbf{k}\|\mathbf{x}$

$$u_{xz}=\tfrac{1}{2}ue^{i(\omega t-kx)}+\text{c.c.} \quad (21)$$

This wave is an external action for the magnetic subsystem in the approximation in which the reaction of the magnetic subsystem to the elastic system is small.

The equation of elasticity in this case has the form

$$\rho\ddot{u}_{xz}=\frac{1}{2}\frac{\partial^2}{\partial x^2}\frac{\partial(F_e+F_{eff})}{\partial u_{xz}}. \quad (22)$$

It is important to take it into account that in a real experiment with a sample of finite dimensions, excitation of transverse strains $u_{xz}(t,x)$ inevitably produces small longitudinal components:

$$u_{xx}=\chi_1u_{xz}, \quad u_{yy}=\chi_2u_{xz}, \quad u_{zz}=\chi_3u_{xz} \quad (\chi_{1,2,3}\ll1). \quad (23)$$

This takes place as a result of the diffraction of the sound beam, and can also occur upon misorientation of the wave vector $\mathbf{k}$ or (and) the polarization $\mathbf{U}$ relative to the x and z axes, respectively (we shall not consider specially chosen beveled crystals in this paper). Solving (22) by the method of slowly changing amplitudes with the boundary condition

$u_{2\omega}|_{x=0} = 0$, and after a number of simple calculations, we obtain the equation for the amplitude of the strain in the second harmonic:

$$u_{2\omega} = \frac{3}{2^4} \frac{k}{C_{55}} B_{55}{}^2 B_\chi \left(\frac{\gamma}{\Omega_1}\right)^4 \left(\frac{H_E}{M_0}\right)^2 u^2 L,$$

(24)

$$B_\chi \equiv (B_{31} - B_{11})\chi_1 + (B_{32} - B_{12})\chi_2 + (B_{33} - B_{13})\chi_3,$$

where L is the length of the sample.

The equation for the amplitude $u_{2\omega}$ of the second harmonic in the c-phase can be obtained by the substitutions $D_3 \leftrightarrow D_1$, $A_1 \leftrightarrow C_1$, $H_z \leftrightarrow -H_x$ in Eqs. (13) and (24).

In the case $H_y \neq 0$ the spin modes are mixed [see Eq. (10)], but in the approximation linear in ψ this does not affect the frequencies of the AFMR, as is easy to show. The ensuing additional contribution (proportional to H_y) to the effective nonlinearity of the elastic subsystem, due to the anharmonism of the magnetoelastic coupling, is small in the ratio $(\Omega_1/\Omega_2)^2 \ll 1$, since it is determined by processes of linear transformation of both the quasiferro- and also the quasiantiferromagnetic branches of the wave spectrum into sound waves.

In principle, another mechanism of effective acoustical nonlinearity is also possible due to the "purely magnetic" anharmonism $F^{(3)}$ (terms of the form $(\mathscr{M}^\eta)^2 \mathscr{L}^\eta$, $(\mathscr{M}^\eta)^2 \mathscr{M}^\xi$ and so on in the free energy) in conjunction with the processes of linear transformation of spin waves into sound-type waves (19). However, as analysis shows, no such mechanism occurs within the framework of the considered model, because of the rather high symmetry of the magnetic and magnetoelastic interactions.

6. DISCUSSION OF THE RESULTS

We first consider the case $H = 0$. The very existence at $H = 0$ of a second-harmonic signal supports the conclusions of the previous section as that longitudinal strains are present in the initial sound wave in addition to the basic shear (u_{xz}) (at least one of the coefficients χ_i in (23) is different from zero). The experimentally observed temperature dependence $u_{2\omega} \propto \Delta T^{-2}$ agrees well with the theoretical formula (24), since the difference of the constants of the anisotropy $(A_1 - C_1)$ is proportional to T near the spin-flip phase transitions, whence it follows that $\Omega_1{}^2 - \Omega_1{}^2{}_{mes} \propto \Delta T$ when account is taken of (13).

We now obtain a numerical estimate of the efficiency $u_{2\omega}/u_\omega$ of the transformation in accord with (24). We set $k \sim 10^3$ cm^{-1}, $C_{55} \sim 10^{12}$ erg/cm^3, $B_{ij} \sim 5 \times 10^7$ erg/cm^3, $H_E/M_0 \sim 10^4$, $L \sim 1$ cm, $\Omega_1/\gamma \sim 3 \times 10^3$ Oe (at $\Delta T = 1$ K), and $u \sim 10^{-6}$. The estimate gives $u_{2\omega}/u_\omega \sim 10^2 \chi$.

Thus, the misorientation of k relative to the a axis by an angle $\chi \sim 1°$, which arises as a result of the diffraction of the sound beam, is quite enough for the explanation of the observed value $u_{2\omega}/u_\omega \sim 1$. This allows us to predict that when specially chosen cuts of the crystal TmFeO$_3$ are used the efficiency of the synchronous generation of the second harmonic should increase by 10–100 times. In particular, for the longitudinal quasisound wave, propagating in the π_1 direction (the notation is that of Ref. 17), an estimate of the pa-

rameter Γ of the effective "phonon-phonon" interaction at $\Delta T \sim 0.1$ K gives $\Gamma \equiv C_3^{eff}/C_2 \sim 10^5$. Such a strong acoustical nonlinearity that depends on the temperature and (or) the magnetic field [see (24)] can be of interest for technical applications.

We now discuss the case $H \neq 0$. The temperature and field dependences of the observed second-harmonic signal $(u_{2\omega} \propto H_y/\Delta T^3)$ suggest the presence of an effective acoustical nonlinearity mechanism that does not find its explanation within the framework of the theoretical model considered. Such a temperature dependence of the second harmonic signal can be explained if we assume the presence in the magnetic energy of an anharmonism of the form

$$F_m^{(3)} = 2M_0 H_y \chi (\mathscr{M}^\eta)^3$$

(25)

(χ is a dimensionless parameter), which, in conjunction with the processes of linear transformation of the spin wave into a sound wave (19) leads to the following expression for the amplitude of the strain in the second harmonic:

$$|u_{2\omega}| = \frac{3}{2^5} \frac{M_0 H_y}{C_{55}} (kL) B_{55}{}^3 \left(\frac{\gamma}{\Omega_1}\right)^6 \left(\frac{H_E}{M_0}\right)^3 \chi u^2.$$

(26)

At typical values of the parameters (see above, as well as $M_0 \approx 420$ Oe and $H_y = 5 \times 10^3$ Oe), the estimate (26) yields $u_{2\omega}/u_\omega \sim 10^5 \chi$.

Thus, in order that the Eq. (26) agree in order of magnitude with the experimental $u_{2\omega}/u_\omega \sim 0.1$ it is necessary that $\chi \sim 10^{-6}$. Against the background of the magnetic anharmonism proper, which determines the interaction of three spin waves of the quasiferromagnetic branch of the spectrum:

$$F_m^{(3)} = -M_0 H_y (\mathscr{M}^\eta)^2 \mathscr{M}^\xi,$$

(27)

which occurs in the nonlinear part of the magnetic energy in the model of a two-sublattice AF (but does not lead to an effective nonlinearity—see the previous section), the anharmonism (25) is smaller by six orders of magnitide. The reason for the appearance of the "purely magnetic" nonlinearity (26) can be the interaction of the subsystem of Fe^{3+} ions with the subsystem of rare-earth ions whose surrounding has a much lower local symmetry.

The features of the behavior of the second-harmonic signal near the transition point can apparently be attributed to the reaction of the second harmonic wave to the primary wave, which becomes important at comparable intensities of the two components. Under these conditions, since the considered waves are propagated with different phase velocities, the $u_{2\omega}$ (u_ω) should have an oscillatory character.[18]

CONCLUSIONS

1. Rare-earth orthoferrites near spin flip are a convenient object for observation and investigation of nonlinear magnetoacoustical effects.

2. Two mechanisms of generation of the second harmonic are delineated: (a) The first, due to the magnetoelastic nonlinearity, is characterized by values of the modulus C_3^{eff} up to 10^{17} erg/cm^3. The value of the doubling effect and its temperature dependence in the absence of a component of

the magnetic field along the "difficult" axis ($H_y = 0$) are well described by the phenomenological theory. b) For the explanation of the second, "purely magnetic" mechanism of nonlinearity, which appears against the background of the first at $H_y \neq 0$, it is necessary to carry out a theoretical analysis on a more complicated model of an antiferromagnetic—evidently with account taken of the effect of the spin subsystem of the rare-earth ions.

3. An anomalous behavior of the signal in the region of strong nonlinearity has been observed, a full explanation of which probably calls for a theory outside the framework of harmonic analysis.

[1]P. P. Maksimenkov and V. I. Ozhogin, Zh. Eksp. Teor. Fiz. **65**, 657 (1973) [Sov. Phys. JETP **38**, 324 (1974)].

[2]V. I. Ozhogin and V. L. Preobrazhenskiĭ, a) Int. Conf. Magn., Abstracts, 3C-9, Amsterdam, 1976; b) Physica **86-88**, 979 (1977), c) Zh. Eksp. Teor. Fiz. **73**, 988 (1977) [Sov. Phys. JETP **46**, 523 (1977)].

[3]J. K. Jao and F. B. Morgenthaler, AIP Conf. Proc. No. **24**, New York 1975, p. 655.

[4]V. I. Ozhogin, A. Yu. Lebedev and A. Yu. Yakubovskiĭ, Pis'ma Zh. Eksp. Teor. Fiz. **27**, 333 (1978) [JETP Lett. **27**, 313 (1978)].

[5]V. L. Preobrazhenskiĭ, M. A. Savchenko, and N. A. Ekonomov, Pis'ma Zh. Eksp. Teor. Fiz. **28**, 93 (1978) [JETP Lett. **28**, 87 (1978)].

[6]V. V. Berezhnov, E. N. Evtikhiev, V. L. Preobrazhenskiĭ, and N. A. Ekonomov, Akust. ZH. **26**, 328 (1980) [Sov. Phys. Acoustics **26**, 180 (1980)].

[7]A. Yu. Lebedev, V. I. Ozhogin, and A. Yu. Yakubovskiĭ, Pis'ma Zh. Eksp. Teor. Fiz. **34**, 22 (1981) [JETP Lett. **34**, 19 (1981)].

[8]G. Gorodetsky, S. Shaft and B. M. Wanklyn, Phys. Rev. **B14**, 2051 (1976).

[9]K. P. Belov, A. K. Zvesdin, A. M. Kadomtseva, and R. Z. Levitin, Usp. Fiz. Nauk **119**, 447 (1976) [Sov. Phys. Uspekhi **19**, 574 (1976)].

[10]F. B. Hagedorn and E. M. Gyorgy, Phys. Rev. **174**, 540 (1968).

[11]R. C. Le Craw, R. Wolfe, E. M. Gyorgy, F. B. Hagedorn, J. C. Hensel, and J. P. Remeika, J. Appl. Phys. **39**, 1019 (1968).

[12]F. B. Hagedorn, E. M. Gyorgy, R. C. Le Craw, J. C. Hensel and J. P. Remeika, Phys. Rev. Lett. **21**, 364 (1968).

[13]A. Yu. Lebedev, V. N. Ozhogin and A. Yu. Yakubovskiĭ, IEEE Tran. on Magnetics, **MAG-17**, 2727 (1981).

[14]E. K. Grishchenko, Akust. Zh. **25**, 44 (1979) [Sov. Phys. Acoustics **25**, 23 (1979)].

[15]Y. Shapira, Phys. Rev. **184**, 589 (1969).

[16]I. E. Dikshteĭn, V. V. Tarasenko and V. G. Shavrov, Fiz. Tverd. Tela **19**, 1107 (1977) [Sov. Phys. Solid State **19**, 644 (1977)].

[17]K. Brugger, J. Appl. Phys. **36**, 759 (1965).

[18]M. B. Vinogradov, O. V. Rudenko and A. P. Sukhorukov, Teoriya voln (Theory of Waves), Moscow, Nauka, 1979, p. 171.

Translated by R. T. Beyer